p38α limits the contribution of MAP17 to cancer progression in breast tumors

Maria V. Guijarro[1], Mar Vergel[2], Juan J. Marin[2,3], Sandra Muñoz-Galván[2], Irene Ferrer[4], Santiago Ramon y Cajal[5], Giovana Roncador[6], Carmen Blanco-Aparicio[7] and Amancio Carnero[2,8,9]

(1) Department of Pathology, New York University School of Medicine, New York NY 10016, USA; (2) Instituto de Biomedicina de Sevilla, IBIS/HUVR. Seville, Spain; (3) Department of Preventive Medicine and Public Health, Seville University, Seville, Spain; (4) Institut d'Investigació Biomédica de Bellvitge-IDIBELL; (5) Pathology Department, Fundacio´ Institut de Recerca Hospital Vall d'Hebron, Barcelona, Spain; (6) Biotechnology Program, Spanish National Cancer Center (CNIO), Madrid, Spain; (7) Experimental Therapeutics, Spanish National Cancer Center (CNIO), Madrid, Spain; and (8) Consejo Superior de Investigaciones Cientificas, Spain

(9)Corresponding author: Amancio Carnero
Instituto de Biomedicina de Sevilla/HUVR, CSIC
Hospital Universitario Virgen del Rocio
Avda. Manuel Siurot s/n
41013, Sevilla, Spain
acarnero@us.es

Running title: MAP17 increases tumor properties of breast carcinoma cells
Key words: breast carcinoma / MAP17 / ROS / p38

ABSTRACT

MAP17 is a small, 17kDa, non-glycosylated membrane protein that is overexpressed in a percentage of carcinomas. In the present work, we have analyzed the role of MAP17 expression during mammary cancer progression. We have found that MAP17 is expresed in 60% human mammary tumors while is not expressed in normal or benign neoplasias. MAP17 levels increased with breast tumor stage and were strongly correlated with mammary tumoral progression. A significant increase in the levels of reactive oxygen (ROS) was observed in MAP17-expressing cells, as compared with parental cells. This increase was further paralleled by an increase in the tumorigenic capacity of carcinoma cells but not in immortal non-tumoral breast epithelial cells, which provides a selective advantage once tumorigenesis has begun. Expression of specific MAP17 shRNA in protein-expressing tumor cells reduced their tumorigenic capabilities, which suggests that this effect is dependent upon MAP17 protein expression. Our data shows that ROS acts as a second messenger that enhances tumoral properties, which are inhibited in non-tumoral cells. We have found that p38α activation mediates this response. MAP17 triggers a ROS-dependent, senescence-like response that is abolished in the absence of p38a activation. Furthermore, in human breast tumors, MAP17 activation is correlated with a lack of phosphorylation of p38α. Therefore, MAP17 is overexpressed in late-stage breast tumors, in which oncogenic activity relies on p38 insensitivity to induced intracellular ROS.

INTRODUCTION

A genome-wide retroviral cDNA screen was conducted to find genes that confer a selective advantage upon cancer cells once tumorigenesis has begun. This screen has allowed us to identify MAP17 (Guijarro *et al.* 2007a), a small, non-glycosylated membrane-associated protein of 17 kDa, which is located on the plasma membrane and the Golgi apparatus (Kocher *et al.* 1995, Kocher *et al.* 1996). The protein sequence possesses a hydrophobic amino-terminus containing 13 amino acids that encodes a PDZ-binding domain and two transmembrane regions (Jaeger *et al.* 2000, Lanaspa *et al.* 2007). MAP17 was first described using differential display overexpression in carcinomas (Kocher *et al.* 1995, Kocher *et al.* 1996). MAP17 binds several PDZ domain-containing proteins, including PDZK1, NHERF proteins, NaPilla and NHe3. Together with NHRF3 and NHRF4, overexpression of MAP17 in opossum kidney cells leads to internalization of NaPilla to the trans-Golgi network (Lanaspa *et al.* 2007) (Pribanic *et al.* 2003). The physiological role of MAP17 in proximal tubules is not known, but it stimulates specific Na-dependent transport of mannose and glucose in *Xenopus* oocytes (Blasco *et al.* 2003) and mammary cells (Guijarro *et al.* 2007a).

Using a melanoma cell model system, we have previously shown that MAP17 enhances tumorigenic properties of melanoma cells through an increase in reactive oxygen species (ROS) (Guijarro *et al.* 2007b). At the molecular level, we have found that MAP17 protects Rat1a fibroblasts from Myc-induced apoptosis through ROS-mediated activation of the PI3K/AKT signaling pathway (Guijarro *et al.* 2007d). In MAP17-overexpressing cells, we showed that a fraction of PTEN undergoes oxidation. Furthermore, activation of AKT by MAP17, as measured by Thr308 phosphorylation, was independent of PI3K activity. Notably, modulation of ROS by antioxidant treatment prevented activation of AKT and restored the level of apoptosis in serum-starved Rat1/c-Myc fibroblasts (Guijarro *et al.* 2007d).

MAP17 is overexpressed in a great variety of human carcinomas (Guijarro *et al.* 2007c). In prostatic and ovarian carcinomas, immunohistochemical analysis of MAP17 during cancer progression shows that its overexpression strongly correlates with tumoral progression (Guijarro *et al.* 2007d). More than 80% of human cancers are carcinomas, and the pattern of expression of MAP17 may be important for understanding the

behaviour of these tumors (Guijarro *et al.* 2007c). Therefore, it is important to determine how MAP17 deregulates carcinoma cell growth.

In the present work, we describe the increase of MAP17 protein levels in a subset of human mammary carcinomas and how MAP17 levels correlated with the progression of human breast tumors. MAP17 enhanced cell prolifferation decreasing doubling time, increases foci formation and growth in soft agar. This increase in the tumorigenic capacities occurs when MAP17 is ectopically expressed in human breast carcinoma cells but not in immortal non-tumoral breast epithelial cells. Moreover, this effect was dependent on the activation of p38α. These results suggest that MAP17 provides a selective advantage once tumorigenesis has begun.

MATERIALS AND METHODS

Cell culture. T47D mammary carcinoma cells were obtained from ATCC and maintained in DMEM with glutamax (Gibco) containing 10% fetal bovine serum (FBS, Sigma), penicillin, streptomycin and fungizone. Cultures were selected when indicated with 75 µg/ml hygromycin (Calbiochem), 400 µg/ml G418 (Sigma) or 2 µg/ml puromycin (Fluka). Human MAP17 full cDNA was cloned in pBabepuro or pWZLhygro, and expressing cultures were generated by retroviral infection. Six mass cultures were selected and tested; all behaved similarly. For this work, 3 representative mass cultures were used in each case. Human mammary epithelial cells, HMECs, (Invitrogen) were infected with retrovirus carrying pBabepuro hTERT (HMEC-Ts), or pBabepuro alone (parental, P). Cells were selected with 2 µg/ml puromycin, and the mass culture was grown for 20 passages (around 40 dounbings) before any other experiments were initiated. Primary and Immortal HMEC-Ts were cultured using standard procedures in HMEC medium (Invitrogen) supplemented with 10% FBS and antibiotics.

Retroviral-Mediated Gene Transfer. Infections were performed as previously indicated by (Carnero *et al.* 2000). Packaging LinXE cells were plated in a 10-cm dish, incubated for 24 h and then transfected by calcium phosphate precipitation with 20 µg of the retroviral plasmid (16 h at 37°C). After 48 h, the virus-containing medium was filtered (0.45-µm filter, Millipore) and supplemented with 8 µg/ml polybrene (Sigma) and an equal volume of fresh medium. Target cells were seeded at 10^6 cells/10-cm dish and incubated overnight. For infections, the culture medium was replaced by the appropriate viral supernatant; the culture plates were centrifuged (1 h, 1,500 rpm) and incubated at 37°C for 16 h. The infected cell population was purified using the appropriate selection.

RT-PCR. Total RNA was purified using TRI-REAGENT (Molecular Research Center, Cincinnati Ohio). Reverse transcription was performed with 5 µg of mRNA using MMLV reverse transcriptase (Promega) and oligodT primer, according to the manufacturer's recommendations. The following primers were used to amplify specific cDNA regions: MAP17 forward 5´-CAGCCATGTCGGCCCTCA-3´ and reverse 5´-TTATTTCACAGAAATTAGGGCC-3´; β-actin: forward 5´-AGGCCAACCGCGAGAAGATGAC-3´ and reverse 5´-GAAGTCCAGGGCGACGTAGCA-3´. The cDNA was subjected to PCR under standard conditions (95ºC 30'', 65ºC 45'', 72ºC 45''; 30 cycles), and products were analyzed by 1% agarose gel electrophoresis.

Surrogate assays

Growth in low serum. A time course curve of parental and MAP17-expressing cells was generated by seeding 10^4 cells in 2.5-cm dishes in triplicate. After 24 h, the medium was changed (day 0), and the indicated culture medium was added. After 4 days, the cells were fixed and stained with crystal violet. After extensive washing, crystal violet was resolubilized in 15% acetic acid and quantified at 595 nm as a relative measure of cell number. Values are expressed as the percentage of cell growth of cells growing in the presence of 10% FBS. Zero percent refers to the number of cells at day 0. Culture media tested were: NS (no serum or complements used, cells were grown in DMEM alone), 0.5 % (DMEM+0.5% FBS), 0.5%+ITS (DMEM + 0.5% FBS + Insulin, transferrin and selenium) and ITS (DMEM + insulin, transferrin and selenium).

Proliferation curve. A total of 10^4 cells were seeded in 2.5-cm plates. The medium was replaced every three days. At the indicated times, the cells were fixed, stained with crystal violet and thoroughly washed.

Clonability. In 10-cm plates, the following quantities of cells were seeded: 10^2, $5x10^2$, 10^3 or 10^4. The medium was replaced every three days, and after 10 days, the cells were fixed and stained with crystal violet. After extensive washing, the colonies were counted. Values are expressed as the percentage of colonies related to the parental cell line.

Growth in soft agar. To measure the anchorage-independent growth, $2x10^4$ cells were suspended in 1.4% agarose D-1 Low EEO (Pronadisa) growth medium containing 10% FBS, disposed onto a solidified base of growth medium containing 2.8% agar and overlaid with 1 ml of growth medium. After 24 h, medium containing 10% FBS was added to each

35-mm dish and replaced twice weekly. Colonies were scored after 3 weeks, and all values were measured in triplicate. Photographs were taken with a phase-contrast microscope (Olympus).

SA ß-Gal activity. Senescence-associated (SA) ß-galactosidase (ß-gal) activity was measured as previously described (Carnero and Beach 2004, Ruiz *et al.* 2008), except that cells were incubated in 5-bromo-4-chloro-3-indolyl-ß-D-galactopyranoside (XGal) at pH 5.5 to increase the sensitivity of the assay. The percentage of cells expressing SA ß-gal was quantified by visual analysis of >400 cells per 10-cm plate in triplicate.

Immunodetection of MAP17. Cells were trypsinized and cytospinned onto glass coverslips. The following day cells were fixed with acetone for 10 min and then incubated with MAP17 monoclonal antibody for 30 min. Cells were washed three times with PBS and incubated for additional 30 min with a secondary goat anti-mouse antibody (DAKO Cytomation) diluted 1:50 in fetal bovine serum. After washing, slides were mounted with Aquatex (Merck). Photos were taken in an Olympus Provis Microscope AX70.

ROS fluorescent detection. To visualize intracellular ROS levels, cells grown on coverslips were washed twice with warm PBS. The cells were then incubated at 37ºC with 8 µM of CM-H_2DCFDA in warm PBS supplemented with 2.5 mM glucose for 15 min. The PBS was then replaced with DMEM supplemented with 10% FBS, and cells were incubated for an additional 10 min under the same conditions. Cells were washed once again with warm PBS and fixed with 4% paraformaldehyde (Sigma) at room temperature for 5 min. The fixed cells were washed three times with PBS, and the coverslips were mounted in Mowiol (Sigma). Intracellular ROS levels were visualized using a confocal ultra-spectral microscope Leica TCS-SP2-AOBS-UV.

Tissue microarray immunohistochemistry

To corroborate the in vitro results, immunohistochemical studies were performed in mammary tumor specimens included in a TMA (tissue microarray). This TMA was constructed using standard methods, which employed paraffin-embedded tumoral samples kindly provided by the Pathology Department at Hospital Vall d'Hebron. Three-micrometer slices were sectioned from the TMA block and applied to special immunochemistry coated slides (DAKO, Glostrup, Denmark). The slides were baked

overnight in a 56ºC oven, deparaffinized in xylene for 20 min, rehydrated through a graded ethanol series and washed with PBS. A heat-induced epitope retrieval step was performed by heating a slide in a solution of sodium citrate buffer pH 6.5 for 2 min in a conventional pressure cooker. After heating, the slide was incubated with proteinase K for 10 min and then rinsed in cool running water for 5 min. Endogenous peroxide activity was quenched with 1.5% hydrogen peroxide (DAKO) in methanol for 10 minutes, and incubation with the primary antibody antiMAP17 (1:250) was performed (40 min). After incubation, immunodetection was carried out with the EnVision (DAKO, Glostrup, Denmark) visualization system using diaminobenzidine chromogen as the substrate, according to manufacturer's instructions. Immunostaining was performed in a TechMate 500 automatic immunostaining device (DAKO).

Antibodies. phospho-p38 MAPK (Thr180/Tyr182) (12F8) rabbit mAb #4631 for IHCh (Cell Signaling); phospho-p38 MAPK (Thr180/Tyr182) (3D7) rabbit mAb for WB (Cell Signaling); phospho-AKT (S473); monoclonal MAP17 antibody, which was generated from bacterial-purified GST-MAP17 protein. Several clonal antibodies were tested for specificity and validated by antigen competition for full characterization).

RESULTS

MAP17 overexpression in human mammary tumors correlates with advanced stages.

MAP17 is overexpressed in carcinomas, specifically in ovarian and prostate carcinomas, in which its overexpression is correlated with advanced stages (Guijarro *et al.* 2007c). Therefore, we first wanted to confirm whether MAP17 expression is a marker for human breast tumors. To assess the overexpression of MAP17 protein, we immunohistochemically analyzed 50 samples from mammary tumors at different stages, including non-tumoral tissues and intraductal neoplasias (MINs) (Fig. 1). To homogenize the results, we generated a tissue array using all the samples. The array was labeled with antiMAP17 antibodies, and the MAP17 levels were independently evaluated (Guijarro *et al.* 2007d). The analysis of the samples showed that MAP17 expression positively correlated with the tumor stage (Fig. 1). Both normal mammary ductal and MIN cells showed no staining for MAP17, which indicates low levels of this protein (Fig. 1). MAP17 expression was detected mainly in carcinomas at stage T2 or T3 s (Fig. 1) (Chi square test, $P<0.0001$).

MAP17 confers a proliferative advantage to breast carcinoma cells but not to non-tumoral immortal epithelial cells.

MAP17 was overexpressed in human mammary carcinomas, and expression was correlated with increased malignancy and tumor grade. Therefore, we next investigated the role of MAP17 in mammary tumorigenesis. To study the biological effect of MAP17 in mammary epithelial cells, we selected cells that do not express MAP17 mRNA. We ectopically expressed the wild-type human MAP17 cDNA and studied the alterations in the biological properties of these cells. We choose HMECs, which are non-tumoral, pre-senescent cells from normal mammary epithelium, and T47D, a tumorigenic mammary carcinoma stablished cell line.

Because HMECs are normal epithelial cells with a limited replicative lifespan (Dimri *et al.* 2005) (Lewis *et al.* 2006) (Stampfer and Yaswen 2000), we first generated an immortal population by expressing the catalytic subunit of telomerase, hTERT (Herbert *et al.* 2002) (Dimri *et al.* 2005, Stampfer and Yaswen 2003). We verified the immortality of the population by maintaining it beyond passage 60 (normal cells enter senescence at approximately passage 10). Immortal HMECs expressing hTERT (HMEC-Ts) were infected with a retrovirus carrying MAP17 cDNA driven by an LTR promoter (Figure 2A). MAP17-expressing cultures grew more slow than parental cells. The doubling time of the MAP17-expressing cultures increased and they ended in arrested state (Figure 2B). We observed that most MAP17-expressing HMEC-Ts stopped growth and changed morphology into a senescence-like state; however, some apoptosis was also observed in the culture (usually less than 10% of cells). These senescent cells also stained for senescence-associated β-gal (Fig. 2C). Our results indicate that MAP17 expression does not induce transforming capabilities in HMEC-Ts.

Because MAP17 is detected only in late-stage breast tumors (Fig. 1), we decided to study the role of MAP17 expression in stablished breast cells that were already tumoral. T47D do not express MAP17 (Guijarro *et al.* 2007c), probably originated from a non-MAP17 expressing tumor. We therefore generated MAP17-expressing T47D cells as before and maintained the subcultivation for short times to avoid culture drift.

We selected several mass cultures and characterized the MAP17 mRNA expression by RT-PCR (Fig. 2C). All the analyzed cultures derived from transfection expressed considerable amounts of MAP17 mRNA, comparable to mass cultures of HMEC-T expressing MAP17 ectopically (supplementary figure 1). MAP17-expressing cells grew faster than parental T47D cells expressing only vector (Figure 2D) and formed more colonies when seeded at low density (Figure 2E). In addition, MAP17-expressing T47D cells formed more colonies when placed in soft agar (Figure 2F, bold bars). Growing in soft agar, MAP17-expressing T47D cells also formed bigger colonies than parental cells (Figure 2E, hatched bars).

Downregulation of MAP17 decreases the malignant behavior of tumor cells.

We have shown that ectopic MAP17 expression increases the tumorigenicity of breast tumor cells. However, it is possible that this result is an indirect effect due to permanent alterations caused by MAP17. To explore this possibility, we studied the prevalence of MAP17-induced properties on further downregulation of MAP17. We expressed specific MAP17 shRNAs in MAP17-expressing T47D cells. We performed the experiments in all MAP17-expressing mass cultures from Figure 2C and obtained results identical to those results shown in Figure 3. In the later figure, we show results from mass cultures expressing MAP17 shRNA derived from MAP17 expressing clone B. The resultant MAP17 shRNA-expressing clones have lost MAP17 expression (Fig. 3A), and this change led to a decrease in colony size and in the number of colonies in both clonability and the soft agar assay (Figs. 3B and 3C). These data indicate that continuous MAP17 expression is required to maintain the increase in oncogenic capabilities.

Next, we analyzed the effect of downregulating endogenous MAP17. We have previously shown that the mammary carcinoma cell line MDA-MB-431 expresses high levels of MAP17 mRNA (Guijarro *et al.* 2007d). Again, MAP17 shRNA reduced the levels of protein, as compared with vector-expressing cells (Fig. 3D). The reduction in the levels of MAP17 is accompanied by a decrease in the proliferation ratio (Figure 3E) and the ability to form colonies at low density (Figure 3F). Moreover, a reduction in MAP17 levels decreased the number and size of colonies growing in soft agar (Fig. 3G and 3H).

The enhanced oncogenic capabilities induced by MAP17 in tumoral cells correlated to an increase of intracellular ROS.

Growing evidence suggests that ROS act as secondary messengers in intracellular signaling cascades that induce and maintain the oncogenic phenotype of tumoral cells. ROS have been shown to induce proliferation, survival and cellular migration (Behrend *et al.* 2003, Martindale and Holbrook 2002, Pelicano *et al.* 2004). We have observed that MAP17 can induce ROS production in Rat1A cells (Guijarro *et al.* 2007e). Therefore, we investigated whether MAP17 expression induces an increase of intracellular ROS in carcinoma cells and whether this increase was responsible for their tumorigenic capabilities.

First, we measured the level of ROS in living cells with the fluorescent probe DCF. MAP17-expressing clones showed higher levels of ROS with respect to their parental counterparts (Fig. 4A) which can be inhibited by ROS scavengers (supplementary figure 2); We also found that ROS increased in HMEC-Ts expressing MAP17(Figure 4A). And Ros scavengers reduced the senescent phenotype observed in HMEC-T expressing MAP17 (supplementary figure 3). ROS was abolished by MAP17shRNA in T47D expressing MAP17 cells, indicating that the effect observed in the clones is due to MAP17 expression (Fig. 4A). Finally, we determined that the expression of shRNA against MAP17 in MDA-MB-431 cells also reduced ROS levels in these cells (Fig. 4B).

Because ROS can act as a secondary messenger (Irani *et al.* 1997), we next checked whether some of the transforming properties of MAP17 were linked to the increased intracellular ROS level. Thus, we examined clonability and growth in soft agar in the presence of antioxidants, such as GSH. We found that the presence of antioxidants reduced the oncogenic properties of the MAP17-expressing cells; they had reduced colony formation efficiency in the presence of antioxidants (Fig. 4C). The same effect was found in the soft agar growth assay; antioxidants reduced the number and size of colonies of MAP17-expressing cells (Fig. 4D-F). Notably, the colony formation efficiency and colony size were similar to untreated parental cells.

Our data indicated that the expression of MAP17 in established human breast cancer cells induces an increase in intracellular ROS levels that plays an important role in

the enhancement of the malignant cell behavior. However, in non-tumoral cells, ROS may have the opposite effect (i.e., inducing cellular senescence).

p38α activation limits MAP17 contribution to progression in breast tumors

Recently, it has been reported that p38α is a sensor for ROS levels and acts as a switch between its oncogenic and suppressive actions (Dolado *et al.* 2007). Inactivation of p38α may be necessary for ROS, and hence MAP17, to enhance tumorigenic properties of the cells. To explore this hypothesis, we first studied the effect of MAP17 expression on p38α phosphorylation at T180/Y182. Ectopic expression of MAP17 induced p38α phosphorylation in HMEC-Ts but not in T47D cells (Fig. 5A). Next, we downregulated p38α in HMEC-Ts by expressing p38α shRNA (Fig. 5B). In these cells, we expressed MAP17 and observed that p38α phosphorylation was not detected (Fig. 5C). In the p38α shRNA expressing cells, MAP17-induced senescence was greatly reduced (Fig. 5D and 5E). HMEC-Ts expressing MAP17 in the absence of p38α then grew faster and formed more colonies when seeded at low density (Fig. 5F and 5G). These results confirm the importance of p38α in mediating the MAP17 effect.

Finally, if p38α limits MAP17-induced enhancement of tumoral properties, we should find a correlation in fresh tumor samples. To investigate this hypothesis, we stained the mammary tumor samples for p38α phosphorylation at T180/Y182. We also stained the samples for AKT phosphorylation at S473 because we have previously shown a functional correlation between MAP17 and AKT activation (Guijarro *et al.* 2007d). Our analysis showed a statistically significant correlation between MAP17 expression and AKT phosphorylation (Fig. 6). We also found a significant correlation between MAP17 expression and a lack of p38α phosphorylation (Fig. 6). Furthermore, tumors not expressing MAP17 showed low levels of AKTS473 and high levels of p38 phosphorylation (Fig. 6).

All these data reinforces the functional relationship between MAP17 and p38α phosphorylation.

DISCUSSION

MAP17 protein is overexpressed in malignant tumors (stages II and II) but not in normal, benign or early stage human breast tumors. Therefore, MAP17 can be

considered an independent marker of malignancy in human breast tumors. We have previously shown that MAP17 overexpression correlates with malignant stages of ovarian and prostate tumors (Guijarro *et al.* 2007c). The relevance of MAP17 as a general marker for the malignant stages of human tumors still needs to be confirmed in other tumors and larger cohorts. However, all tissues explored thus far have shown similar patterns of MAP17 expression. Furthermore, MAP17 expression seems to correlate with AKT473 phosphorylation and a p38T180/Y182 dephosphorylated stage. These expression patterns provide a mechanistic insight (p38 desensitization) and a possible target for future therapies (AKT inhibition).

Carcinoma cells, but not non-tumoral epithelial cells, which stably express MAP17, show an increased tumoral phenotype. This phenotypic change included enhanced proliferative capabilities in both the presence and the absence of cell contact. The increased tumorigenic properties induced by MAP17 are associated with an increase in ROS. This increase is because MAP17 increases endogenous ROS, and the antioxidant treatment of MAP17-expressing cells entails a reduction in the tumorigenic properties of these cells. Thus, ROS generated in a MAP17-dependent manner function as intracellular signals and induce a growth-related program. Accumulating evidence implicates ROS in signaling cascades related to cell proliferation and transformation (Irani *et al.* 1997) (Sundaresan *et al.* 1995) (Burdon 1996) (Church *et al.* 1993, Yan *et al.* 1996) (Fernandez-Pol *et al.* 1982) (Arnold *et al.* 2001, Bae *et al.* 1999).

Oxidative stress has been considered to be a byproduct of cellular metabolism. However, ROS may be involved in the regulation of signal transduction pathways (Hancock *et al.* 2001) (Apel and Hirt 2004) (Yoon *et al.* 2002). ROS can also cooperate with other oncogenic signals in cellular transformation and cancer (Suh *et al.* 1999) (Woo and Poon 2004). The pro-tumoral effects by ROS, including gene expression regulation (Allen and Tresini 2000), increased mutagenic rates (Irani *et al.* 1997) and genomic instability (Woo and Poon 2004) may occur at different levels. High levels of ROS have been detected in cancer cell lines and tumors from different tissues (Szatrowski and Nathan 1991) (Toyokuni *et al.* 1995) (Fernandez-Pol *et al.* 1982), supporting the causal link between oxidative stress and cancer (Ames 1983) (Wagner and Nebreda 2009) (Cuadrado and Nebreda 2010).

ROS increases are sensed by p38α, and activation of p38 α limits the oncogenic capability of MAP17 by driving these cells to senescence or apoptosis. This senescence induction may explain why MAP17 does not induce tumorigenic transformation in immortal non-tumoral cells. In these cells, ROS are probably sensed as pernicious stress rather than as second messengers. The reduction in proliferative capabilities observed in HMEC-Ts supports this hypothesis. Downregulation of p38α prevents the cells from responding to MAP17-induced stress. Therefore, p38α is a sensor of ROS and acts as a switch between ROS pro-oncogenic and tumor-suppressive capabilities (Wagner and Nebreda 2009) (Cuadrado and Nebreda 2010). Furthermore, the inactivation of the p38α response is necessary for ROS, and hence MAP17, to enhance the tumorigenic capabilities of cells. Therefore, cells with impaired p38a response to ROS are more susceptible of being oncogenically altered by MAP17 (see also supplementary figure 4).

In addition to its role in coordinating the stress response, p38α also regulates other cellular processes in a cell-type specific manner (Adams *et al.* 2000, Nebreda and Porras 2000). p38α negatively regulates the malignant transformation induced by oncogenic Ras, even in the absence of functional p53 response (Dolado *et al.* 2007). Different mechanisms have been proposed to explain this tumor suppressive role, including the activation of p53-dependent cell cycle arrest (Bulavin *et al.* 2002), induction of premature senescence (Wang *et al.* 2002) and upregulation of cell cycle inhibitors, such as p16 and p21 (Bulavin and Fornace 2004) (Nicke *et al.* 2005). However, p38α is not a general inhibitor of oncogenic transformation; it specifically modulates malignant transformations induced by oncogenes that produce ROS (Dolado *et al.* 2007). Notably, some human cancer cells can bypass the inhibitory role of p38α on ROS accumulation, and this leads to enhanced tumorigenicity. Thus, oxidative stress detected by p38α is an important mechanism that negatively regulates the onset of cancer. Therefore, p38α limits MAP17-induced enhancement of tumoral properties in mammary tumor cells.

The signaling pathways that lead to the activation of p38 involve several upstream kinases, including ASK1 (MAP3K5), which plays a major role in p38α activation by oxidative stress (Tobiume *et al.* 2001). ASK1 activation may involve oligomerization and autophosphorylation. In unstressed cells, this activation is prevented by the binding of proteins, such as thioredoxin and Gstm1, which are sensitive to stress and dissociate from

ASK1 after oxidative stress and heat shock, respectively (Dorion *et al.* 2002) (Matsukawa *et al.* 2004).

MAP17-induced ROS may oxidize certain cysteine residues of thioredoxin and induce its dissociation from ASK1. This action would induce the activation of the JNK and p38 pathways. MAP17 oncogenic abilities would only be reflected in cell lines that have acquired the ability to uncouple p38α activation from oxidative stress production, resulting in enhanced tumorigenicity. In many cases, this mechanism relies on the ability of the GST family members Gstm1 and Gstm2 to impair p38a activation in response to ROS accumulation (Dorion *et al.* 2002).

ROS can also directly modify signaling proteins through modifications such as nitrosylation, carbonylation, disulfide bond formation and glutathionylation (England and Cotter 2005). A direct effect has been shown on the protein tyrosine phosphatase-1B (PTP-1B), which is inhibited by oxidation of a thiol in the active site (Barrett *et al.* 1999, Lee *et al.* 1998), leading to increased phosphotyrosines on many cell proteins. We have also previously shown that MAP17-induced ROS activate the PI3K pathway. This activation likely occurs through direct oxidation and inactivation of PTEN and other AKT phosphatases, and AKT activation is maintained, even in the absence of PI3K signal (Guijarro *et al.* 2007d). AKT pathway activation induced by MAP17 expression may explain some of the properties described here. Under certain conditions, an increase in AKT activity may lead to a decrease in p38 phosphorylation; a decrease in AKT may lead to an increase in p38α phosphorylation, possibly through the release of the activity of p38 upstream kinases (most likely ASK1 and MEKK3) (Samanta *et al.* 2009). This relationship is further supported by the strong direct correlation between MAP17 levels and AKT phosphorylation and by the p38α dephosphorylation in breast tumors found in this work (Figure 7) and by others (Huang *et al.* 2003). Furthermore, AKT activation may be involved in promoting survival of cells defective for p38 (Zuluaga *et al.* 2007) and in the increase of tumorigenic properties (Carnero 2010). However, we suggest that other pathways induced by MAP17 could coexist at the transcriptional level, as has been described in other systems (Droge 2002, Klaunig *et al.* 1998).

In summary, MAP17 is a biomarker of malignant stages of breast tumors, in which it can enhance tumorigenic properties through ROS. Moreover, p38α limits the contribution of MAP17 in advancing the malignant state of breast tumors.

ACKNOWLEDGMENTS

We wish to thank Augusto Silva and Ricardo Sanchez Prieto for their critical reading of the manuscript and valuable suggestions. This work was supported by grants from the Spanish Ministry of Science and Innovation (SAF2009-08605), Consejeria de Ciencia e Innovacion and Consejeria de Salud of the Junta de Andalucia (CTS-6844 and PI-0142). AC's laboratory is also funded by a fellowship from the Fundacion Oncologica FERO, supported by Fundació Josep Botet.

Conflict of interest

The authors declare no conflict of interest. The funders had no role in study design, data collection and analysis, decision to publish, or preparation of the manuscript.

FIGURE LEGENDS

Figure 1: Robust expression of MAP17 in human breast tumors correlates with advanced stage. A) Correlation of tumor stage with levels of MAP17. After double-blind individual scoring, MAP17 levels were correlated with the tumor stage of the sample using an ANOVA test. **B) Representative pictures of MAP17-stained breast tumors at different stages.**

Figure 2: MAP17 expression enhances the tumorigenic properties of T47D tumor cells but does not induce tumorigenicity in immortal HMECs: A) Characterization of HMEC-Ts MAP17 expressing clones by RT-PCR. HMEC-Ts breast cancer cells were infected with retrovirus carrying human MAP17 cDNA in pBabepuro vector or vector alone. Individual clones were selected and analyzed for MAP17 mRNA expression by RT-PCR. Three representative clones (A, B and C) and parental cells that were infected with vector alone (P) are shown. **B) Growth curve.** A growth curve of HMEC-Ts expressing ectopic MAP17 cDNA (cultures 1, 2 and 3) or vector alone (P) was constructed. Data presented are the mean and standard deviations from two independent experiments performed in triplicate. **C) Characterization of MAP17-expressing clones by SA β–Gal staining.** Immortal non-tumoral HMEC-Ts were infected with retrovirus carrying either human MAP17 cDNA in a pBabepuro vector or vector alone. After puromycin selection (2 μg/ml), the cells were cultured for 4 days, and the SA-β-gal marker was analyzed as indicated in the M&M section. **D) Characterization of T47D-MAP17 expressing clones by RT-PCR.** T47D breast cancer cells were infected with retrovirus carrying human MAP17 cDNA in pBabepuro vector or vector alone. Individual clones were selected and analyzed for MAP17 mRNA expression by RT-PCR. Three representative clones (B, C and E) and parental cells that were infected with vector alone (P) are shown. **E) Growth curve.** A growth curve of T47D cells expressing ectopic MAP17 cDNA (clones B, C and E) or vector alone (P) was constructed. Data presented are the mean and standard deviation from three independent experiments. **F) MAP17 increases the survival of cells seeded at very low density.** Cells (10^3) were seeded in 10-cm dishes in triplicate, grown for 10 days, fixed and stained with crystal violet; then, the number of colonies was counted. Three representative clones (B, C and E) and parental cells (P) are shown. Data presented are the mean

from triplicate experiments (bars ± SD). **G) MAP17 expression increases colony number and size in soft agar.** Cells (10^4) were cultured in soft agar for 4 weeks and then fixed, after which pictures were taken. Data from 3 representative clones (B, C and E) and parental cells (P) are shown. Data presented are the mean from triplicate experiments (bars ± SD). Colony size was determined by measuring a minimum of 30 representative colonies.

Figure 3: Downregulation of MAP17 through shRNA reduces tumorigenic properties. A) MAP17 shRNA reduces protein levels. T47D breast cancer cells expressing ectopic MAP17 cDNA (clone B from Fig 2) were infected with retrovirus carrying MAP17 shRNA (B-sh1, B-sh2, B-sh3) or vector alone (C). Cells were selected and analyzed for MAP17 protein expression by immunodetection after cytospin centrifugation on slides. **B) Downregulation of MAP17 decreases survival of cells seeded at very low density.** Cells (10^3) were seeded in 10-cm dishes in triplicate and grown for 10 days. Cells were then fixed and stained with crystal violet, and the number of colonies was counted. T47D breast cancer cells expressing ectopic MAP17 cDNA (clone B from Fig 2) were infected with retrovirus carrying MAP17 shRNA (B-sh1, B-sh2, B-sh3) or vector alone (C). Cells were selected and analyzed for MAP17, and T47D cells expressing only vector (P) are shown. Data presented are the mean from triplicate experiments (± StDev). **C) Downregulation of MAP17 expression decreases colony number and size in soft agar.** Cells (10^4) were cultured in soft agar for 4 weeks. T47D breast cancer cells expressing ectopic MAP17 cDNA (clone B from Fig 2) were infected with retrovirus carrying MAP17 shRNA (B-sh1, B-sh2, B-sh3) or vector alone (C). Cells were selected and analyzed for MAP17, and T47D cells expressing only vector (P) are shown. Data presented are the mean from triplicate experiments (bars ± SD). Colony size was determined by measuring a minimum of 30 representative colonies. **D) MAP17 shRNA reduces protein levels.** MDA-MB-431 breast cancer cells expressing MAP17 shRNA (sh1, sh2, sh3) or vector alone (P) were selected and analyzed for MAP17 protein expression by immunodetection after cytospin centrifugation on slides. **E) Growth curve.** A growth curve of MDA-MB-431 breast cancer cells expressing MAP17 shRNA (sh1, sh2, sh3) or vector alone (C) was constructed. Data presented are the mean and standard deviation from three independent experiments. **F) Downregulation of MAP17 decreases survival of cells seeded at very low density.** A total of 10^3 MDA-MB-431 breast cancer cells expressing MAP17 shRNA (sh1, sh2, sh3) or vector alone (C) were seeded in 10-cm dishes in triplicate and grown for 10 days. The cells were then

fixed and stained with crystal violet, and the number of colonies was counted. Data presented are the mean from triplicate experiments (bars ± SD). **G, H) Downregulation of MAP17 expression decreases colony number and size in soft agar.** MDA-MB-431 breast cancer cells (10^4) expressing MAP17 shRNA (sh1, sh2, sh3) or vector alone (C) were cultured in soft agar for 4 weeks. Cells were then fixed, and pictures were taken (g). Data presented (h) are the mean from triplicate experiments (bars ± SD). Colony size was determined by measuring a minimum of 30 representative colonies.

Figure 4: MAP17-enhanced tumorigenicity depends on an intracellular increase in ROS. A) MAP17 increases ROS. To visualize intracellular ROS levels, T47D parental or HMEC-T (v) or MAP17-expressing cells (MAP17wt) were grown on coverslips and then incubated at 37°C with 8 μM of CM-H_2DCFDA. Intracellular ROS were visualized using a confocal ultra-spectral microscope (Leica TCS-SP2-AOBS-UV). A representative picture of MAP17-expressing clones and parental cells is shown. As control we shown that downregulation of MAP17 by shRNA (MAP17wt+shMAP17) in T47D ectopically expressing MAP17 (MAP17wt) reduces levels of ROS. **B) Downregulation of MAP17 by shRNA reduces ROS in cells expressing MAP17.** MDA-MB-431 cells carrying vector alone (p) or expressing MAP17 shRNA were analyzed for intracellular ROS levels, as previously described. **C) MAP17 enhances cell survival through ROS production.** Colony number was calculated as follows: triplicate cell samples were cultured for 10 days in the presence or absence of 10 mM GSH; cells were fixed and stained with crystal violet following the protocol described in the M&M; and the number of colonies was counted. 2 representative clones (B and C) and parental cells (P) are shown. Data presented are the mean from triplicate samples (bars ± SD). **D, E and F) MAP17 increases colony number and size in soft agar through ROS production. D)** Pictures of resulting colonies are shown. Cells were grown in the presence or absence of 10 mM GSH for 4 weeks and then fixed, and the number of colonies was counted. **E)** Presented data are the mean from three independent experiments (bars ± SD). 2 representative clones (B and C) and parental cells (P) are shown. **F)** Colony size was determined by measuring a minimum of 30 representative colonies. Presented data are the mean from three independent experiments (bars ± SD). 2 representative clones (B and C) and parental cells (P) are shown.

Figure 5: MAP17 activity is dependent on p38α inactivation. A) MAP17 induces p38α phosphorylation. Indicated cells (HMEC-T or T47D) expressing empty vector (V) or MAP17 cDNA (M17) were grown in the presence of 10% FBS. At 90% confluence the cells were harvested and protein extracted. Total protein was resolved using PAGE, and p38α phosphorylated at T180/Y182 ($p38\alpha^P$), or p38α total protein (p38α) examined using western blot. The experiment was performed more than three independent times, with similar results. **B) p38 shRNA reduces p38 levels.** HMEC-T cells expressing empty vector (V) or p38a shRNA (sh) were grown in the presence of 10% FBS. At 90% confluence the cells were harvested and protein extracted. Total protein was resolved using PAGE, and tubulin or p38α total protein (p38α) examined using western blot. The experiment was performed more than three independent times, with similar results. **C) Downregulation of p38α inhibits its MAP17-induced phosphorylation.** T47D cells expressing MAP17 CDNA (see fig 5A) were transfected with empty vector (V) or p38α shRNA (sh). After selection, cells were grown in the presence of 10% FBS. At 90% confluence the cells were harvested and protein extracted. Total protein was resolved using PAGE, and tubulin or p38α total protein (p38α) examined using western blot. Parental T47D cells not expressing MAP17 are shown as control (C) The experiment was performed more than three independent times, with similar results. **D) Expression of MAP17 mRNA in different cultures expressing p38shRNA.** HMEC-T cells expressing p38a shRNA (see fig 5B) were transfected with MAP17 cDNA. After selection several mass cultures were selected and grown. 3 of these clones were selected for further experiments (mass cultures 1, 2 and 3). Figure shows expression of MAP17 mRNA identified by RT-PCR in these clones. Lane V shows HMEC-T cells expressing empty vector. **E) Downregulation of p38α inhibits MAP17-induced senescence in HMEC-Ts.** HMEC-T cells expressing p38a shRNA obtained in 5D were infected with retrovirus carrying MAP17 cDNA and grown for 4 days in the presence of selection. After that time SA-βgal as measure of cell senescence was analized. Figure shows % of senescent cells identified in each culture. C: HMEC-T with MAP17 cDNA; V: HMEC-T cells expressing empty vector for shRNA and MAP17 cDNA; 1,2 and 3: different mass cultures of HMEC-T expressing p38α shRNA and MAP17cDNA.

F) Downregulation of p38a enhances growth rate of MAP17-expressing HMECs. Time course of HMEC-T cells expressing p38α shRNA infected with retrovirus carrying MAP17 cDNA and grown. At different times the relative number of cells was analized. Figure shows growth courve of mean of 3 independent experiments performed in triplicate.

C: HMEC-T with MAP17 cDNA; V: HMEC-T cells expressing empty vector for shRNA and MAP17 cDNA; 1,2 and 3: different mass cultures of HMEC-T expressing p38a shRNA and MAP17cDNA. **G) Downregulation of p38α enhances colony formation in MAP17-expressing HMECs.** Colony number of HMEC-T cells expressing p38α shRNA infected with retrovirus carrying MAP17 cDNA and grown at low density. Figure shows the number of colonies per 10 cm dish mean of 3 independent experiments performed in triplicate. C: HMEC-T with MAP17 cDNA; V: HMEC-T cells expressing empty vector for shRNA and MAP17 cDNA; 1,2 and 3: different mass cultures of HMEC-T expressing p38α shRNA and MAP17cDNA.

Figure 6: Expression of MAP17 in breast tumors correlates with p38 dephosphorylation at T180/Y182 and AKT phosphorylation at S473. A) Representative pictures of MAP17, AKT473 and p38 T180/Y182 staining in 2 independent tumor samples. B) Correlation of levels of MAP17 with the absence of p38 T102/Y103 staining. After double-blind individual scoring, MAP17 levels were correlated with the tumor stage of the sample using an ANOVA test.

REFERENCES

Adams RH, Porras A, Alonso G, Jones M, Vintersten K, Panelli S *et al* (2000). Essential role of p38alpha MAP kinase in placental but not embryonic cardiovascular development. *Mol Cell* **6:** 109-116.

Allen RG, Tresini M (2000). Oxidative stress and gene regulation. *Free Radic Biol Med* **28:** 463-499.

Ames BN (1983). Dietary carcinogens and anticarcinogens. Oxygen radicals and degenerative diseases. *Science* **221:** 1256-1264.

Apel K, Hirt H (2004). Reactive oxygen species: metabolism, oxidative stress, and signal transduction. *Annu Rev Plant Biol* **55:** 373-399.

Arnold RS, Shi J, Murad E, Whalen AM, Sun CQ, Polavarapu R *et al* (2001). Hydrogen peroxide mediates the cell growth and transformation caused by the mitogenic oxidase Nox1. *Proc Natl Acad Sci U S A* **98:** 5550-5555.

Bae GU, Seo DW, Kwon HK, Lee HY, Hong S, Lee ZW *et al* (1999). Hydrogen peroxide activates p70(S6k) signaling pathway. *J Biol Chem* **274:** 32596-32602.

Barrett WC, DeGnore JP, Konig S, Fales HM, Keng YF, Zhang ZY *et al* (1999). Regulation of PTP1B via glutathionylation of the active site cysteine 215. *Biochemistry* **38:** 6699-6705.

Behrend L, Henderson G, Zwacka RM (2003). Reactive oxygen species in oncogenic transformation. *Biochem Soc Trans* **31:** 1441-1444.

Blasco T, Aramayona JJ, Alcalde AI, Catalan J, Sarasa M, Sorribas V (2003). Rat kidney MAP17 induces cotransport of Na-mannose and Na-glucose in Xenopus laevis oocytes. *Am J Physiol Renal Physiol* **285:** F799-810.

Bulavin DV, Amundson SA, Fornace AJ (2002). p38 and Chk1 kinases: different conductors for the G(2)/M checkpoint symphony. *Curr Opin Genet Dev* **12:** 92-97.

Bulavin DV, Fornace AJ, Jr. (2004). p38 MAP kinase's emerging role as a tumor suppressor. *Adv Cancer Res* **92:** 95-118.

Burdon RH (1996). Control of cell proliferation by reactive oxygen species. *Biochem Soc Trans* **24:** 1028-1032.

Carnero A, Hudson JD, Hannon GJ, Beach DH (2000). Loss-of-function genetics in mammalian cells: the p53 tumor suppressor model. *Nucleic Acids Res* **28:** 2234-2241.

Carnero A, Beach DH (2004). Absence of p21WAF1 cooperates with c-myc in bypassing Ras-induced senescence and enhances oncogenic cooperation. *Oncogene* **23:** 6006-6011.

Carnero A (2010). The PKB/AKT pathway in cancer. *Curr Pharm Des* **16:** 34-44.

Cuadrado A, Nebreda AR (2010). Mechanisms and functions of p38 MAPK signalling. *Biochem J* **429:** 403-417.

Church SL, Grant JW, Ridnour LA, Oberley LW, Swanson PE, Meltzer PS *et al* (1993). Increased manganese superoxide dismutase expression suppresses the malignant phenotype of human melanoma cells. *Proc Natl Acad Sci U S A* **90:** 3113-3117.

Dimri G, Band H, Band V (2005). Mammary epithelial cell transformation: insights from cell culture and mouse models. *Breast Cancer Res* **7:** 171-179.

Dolado I, Swat A, Ajenjo N, De Vita G, Cuadrado A, Nebreda AR (2007). p38alpha MAP kinase as a sensor of reactive oxygen species in tumorigenesis. *Cancer Cell* **11:** 191-205.

Dorion S, Lambert H, Landry J (2002). Activation of the p38 signaling pathway by heat shock involves the dissociation of glutathione S-transferase Mu from Ask1. *J Biol Chem* **277:** 30792-30797.

Droge W (2002). Free radicals in the physiological control of cell function. *Physiol Rev* **82:** 47-95.

England K, Cotter TG (2005). Direct oxidative modifications of signalling proteins in mammalian cells and their effects on apoptosis. *Redox Rep* **10:** 237-245.

Fernandez-Pol JA, Hamilton PD, Klos DJ (1982). Correlation between the loss of the transformed phenotype and an increase in superoxide dismutase activity in a revertant subclone of sarcoma virus-infected mammalian cells. *Cancer Res* **42:** 609-617.

Guijarro MV, Castro ME, Romero L, Moneo V, Carnero A (2007a). Large scale genetic screen identifies MAP17 as protein bypassing TNF-induced growth arrest. *J Cell Biochem*.

Guijarro MV, Leal JF, Blanco-Aparicio C, Alonso S, Fominaya J, Lleonart M *et al* (2007b). MAP17 enhances the malignant behavior of tumor cells through ROS increase. *Carcinogenesis* **28:** 2096-2104.

Guijarro MV, Leal JF, Fominaya J, Blanco-Aparicio C, Alonso S, Lleonart M *et al* (2007c). MAP17 overexpression is a common characteristic of carcinomas. *Carcinogenesis* **28:** 1646-1652.

Guijarro MV, Link W, Rosado A, Leal JF, Carnero A (2007d). MAP17 inhibits Myc-induced apoptosis through PI3K/AKT pathway activation. *Carcinogenesis* **28:** 2443-2450.

Hancock JT, Desikan R, Neill SJ (2001). Hydrogen peroxide and nitric oxide in plant defence: revealing potential targets for oxidative stress tolerance? *Biofactors* **15:** 99-101.

Herbert BS, Wright WE, Shay JW (2002). p16(INK4a) inactivation is not required to immortalize human mammary epithelial cells. *Oncogene* **21:** 7897-7900.

Huang E, Cheng SH, Dressman H, Pittman J, Tsou MH, Horng CF *et al* (2003). Gene expression predictors of breast cancer outcomes. *Lancet* **361:** 1590-1596.

Irani K, Xia Y, Zweier JL, Sollott SJ, Der CJ, Fearon ER *et al* (1997). Mitogenic signaling mediated by oxidants in Ras-transformed fibroblasts. *Science* **275:** 1649-1652.

Jaeger C, Schaefer BM, Wallich R, Kramer MD (2000). The membrane-associated protein pKe#192/MAP17 in human keratinocytes. *J Invest Dermatol* **115:** 375-380.

Klaunig JE, Xu Y, Isenberg JS, Bachowski S, Kolaja KL, Jiang J *et al* (1998). The role of oxidative stress in chemical carcinogenesis. *Environ Health Perspect* **106 Suppl 1:** 289-295.

Kocher O, Cheresh P, Brown LF, Lee SW (1995). Identification of a novel gene, selectively up-regulated in human carcinomas, using the differential display technique. *Clin Cancer Res* **1:** 1209-1215.

Kocher O, Cheresh P, Lee SW (1996). Identification and partial characterization of a novel membrane-associated protein (MAP17) up-regulated in human carcinomas and modulating cell replication and tumor growth. *Am J Pathol* **149:** 493-500.

Lanaspa MA, Giral H, Breusegem SY, Halaihel N, Baile G, Catalan J *et al* (2007). Interaction of MAP17 with NHERF3/4 induces translocation of the renal Na/Pi IIa transporter to the trans-Golgi. *Am J Physiol Renal Physiol* **292:** F230-242.

Lee SR, Kwon KS, Kim SR, Rhee SG (1998). Reversible inactivation of protein-tyrosine phosphatase 1B in A431 cells stimulated with epidermal growth factor. *J Biol Chem* **273:** 15366-15372.

Lewis CM, Herbert BS, Bu D, Halloway S, Beck A, Shadeo A *et al* (2006). Telomerase immortalization of human mammary epithelial cells derived from a BRCA2 mutation carrier. *Breast Cancer Res Treat* **99:** 103-115.

Martindale JL, Holbrook NJ (2002). Cellular response to oxidative stress: signaling for suicide and survival. *J Cell Physiol* **192:** 1-15.

Matsukawa J, Matsuzawa A, Takeda K, Ichijo H (2004). The ASK1-MAP kinase cascades in mammalian stress response. *J Biochem* **136:** 261-265.

Moneo V, Serelde BG, Fominaya J, Leal JF, Blanco-Aparicio C, Romero L *et al* (2007). Extreme sensitivity to Yondelis(R) (Trabectedin, ET-743) in low passaged sarcoma cell lines correlates with mutated p53. *J Cell Biochem* **100:** 339-348.

Nebreda AR, Porras A (2000). p38 MAP kinases: beyond the stress response. *Trends Biochem Sci* **25:** 257-260.

Nicke B, Bastien J, Khanna SJ, Warne PH, Cowling V, Cook SJ *et al* (2005). Involvement of MINK, a Ste20 family kinase, in Ras oncogene-induced growth arrest in human ovarian surface epithelial cells. *Mol Cell* **20:** 673-685.

Pelicano H, Carney D, Huang P (2004). ROS stress in cancer cells and therapeutic implications. *Drug Resist Updat* **7:** 97-110.

Pribanic S, Gisler SM, Bacic D, Madjdpour C, Hernando N, Sorribas V *et al* (2003). Interactions of MAP17 with the NaPi-IIa/PDZK1 protein complex in renal proximal tubular cells. *Am J Physiol Renal Physiol* **285:** F784-791.

Ruiz L, Traskine M, Ferrer I, Castro E, Leal JF, Kaufman M *et al* (2008). Characterization of the p53 response to oncogene-induced senescence. *PLoS ONE* **3:** e3230.

Samanta AK, Huang HJ, Le XF, Mao W, Lu KH, Bast RC, Jr. *et al* (2009). MEKK3 expression correlates with nuclear factor kappa B activity and with expression of antiapoptotic genes in serous ovarian carcinoma. *Cancer* **115:** 3897-3908.

Stampfer MR, Yaswen P (2000). Culture models of human mammary epithelial cell transformation. *J Mammary Gland Biol Neoplasia* **5:** 365-378.

Stampfer MR, Yaswen P (2003). Human epithelial cell immortalization as a step in carcinogenesis. *Cancer Lett* **194:** 199-208.

Suh YA, Arnold RS, Lassegue B, Shi J, Xu X, Sorescu D *et al* (1999). Cell transformation by the superoxide-generating oxidase Mox1. *Nature* **401:** 79-82.

Sundaresan M, Yu ZX, Ferrans VJ, Irani K, Finkel T (1995). Requirement for generation of H2O2 for platelet-derived growth factor signal transduction. *Science* **270:** 296-299.

Szatrowski TP, Nathan CF (1991). Production of large amounts of hydrogen peroxide by human tumor cells. *Cancer Res* **51:** 794-798.

Tobiume K, Matsuzawa A, Takahashi T, Nishitoh H, Morita K, Takeda K *et al* (2001). ASK1 is required for sustained activations of JNK/p38 MAP kinases and apoptosis. *EMBO Rep* **2:** 222-228.

Toyokuni S, Okamoto K, Yodoi J, Hiai H (1995). Persistent oxidative stress in cancer. *FEBS Lett* **358:** 1-3.

Wagner EF, Nebreda AR (2009). Signal integration by JNK and p38 MAPK pathways in cancer development. *Nat Rev Cancer* **9:** 537-549.

Wang W, Chen JX, Liao R, Deng Q, Zhou JJ, Huang S *et al* (2002). Sequential activation of the MEK-extracellular signal-regulated kinase and MKK3/6-p38 mitogen-activated protein kinase pathways mediates oncogenic ras-induced premature senescence. *Mol Cell Biol* **22:** 3389-3403.

Woo RA, Poon RY (2004). Activated oncogenes promote and cooperate with chromosomal instability for neoplastic transformation. *Genes Dev* **18:** 1317-1330.

Yan T, Oberley LW, Zhong W, St Clair DK (1996). Manganese-containing superoxide dismutase overexpression causes phenotypic reversion in SV40-transformed human lung fibroblasts. *Cancer Res* **56:** 2864-2871.

Yoon SO, Yun CH, Chung AS (2002). Dose effect of oxidative stress on signal transduction in aging. *Mech Ageing Dev* **123:** 1597-1604.

Zuluaga S, Alvarez-Barrientos A, Gutierrez-Uzquiza A, Benito M, Nebreda AR, Porras A (2007). Negative regulation of Akt activity by p38alpha MAP kinase in cardiomyocytes involves membrane localization of PP2A through interaction with caveolin-1. *Cell Signal* **19:** 62-74.

Figure 1

A

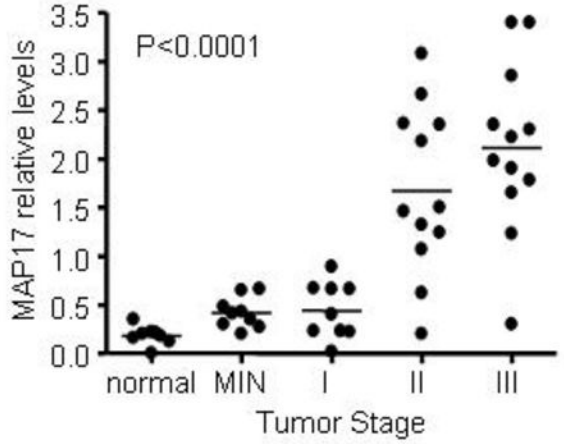
P<0.0001
MAP17 relative levels
3.5
3.0
2.5
2.0
1.5
1.0
0.5
0.0
normal
MIN
I
II
III
Tumor Stage

B

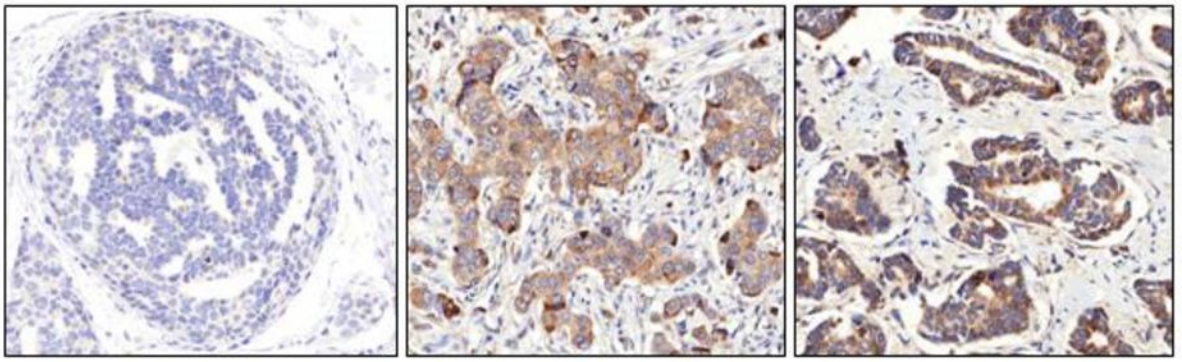

Figure 2

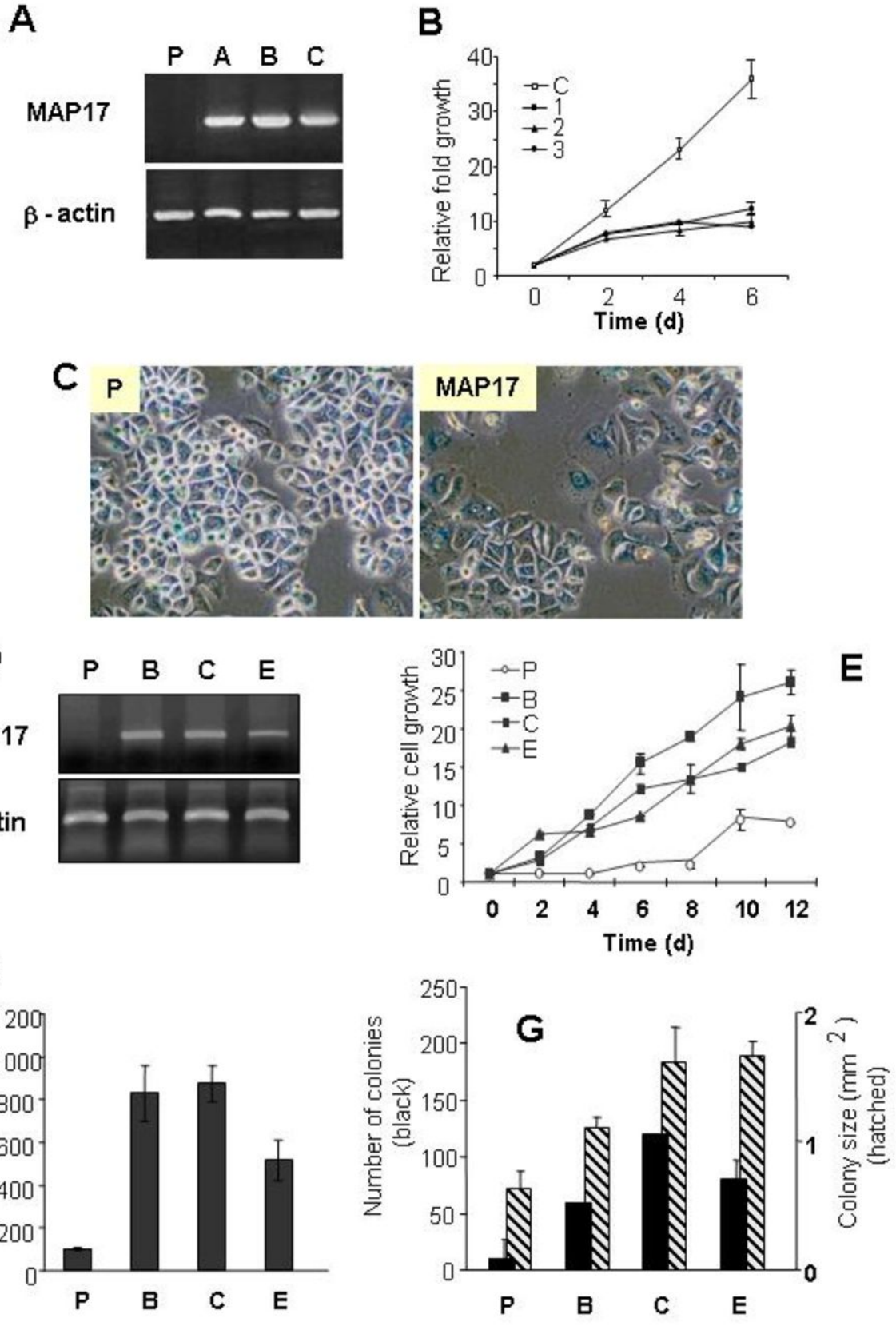
A
P A B C
MAP17
β - actin
B
Relative fold growth
C
1
2
3
Time (d)
C
P
MAP17
D
P B C E
MAP17
β-actin
E
Relative cell growth
P
B
C
E
Time (d)
F
Relative number of colonies (%)
P B C E
G
Number of colonies (black)
Colony size (mm 2) (hatched)
P B C E

Figure 3

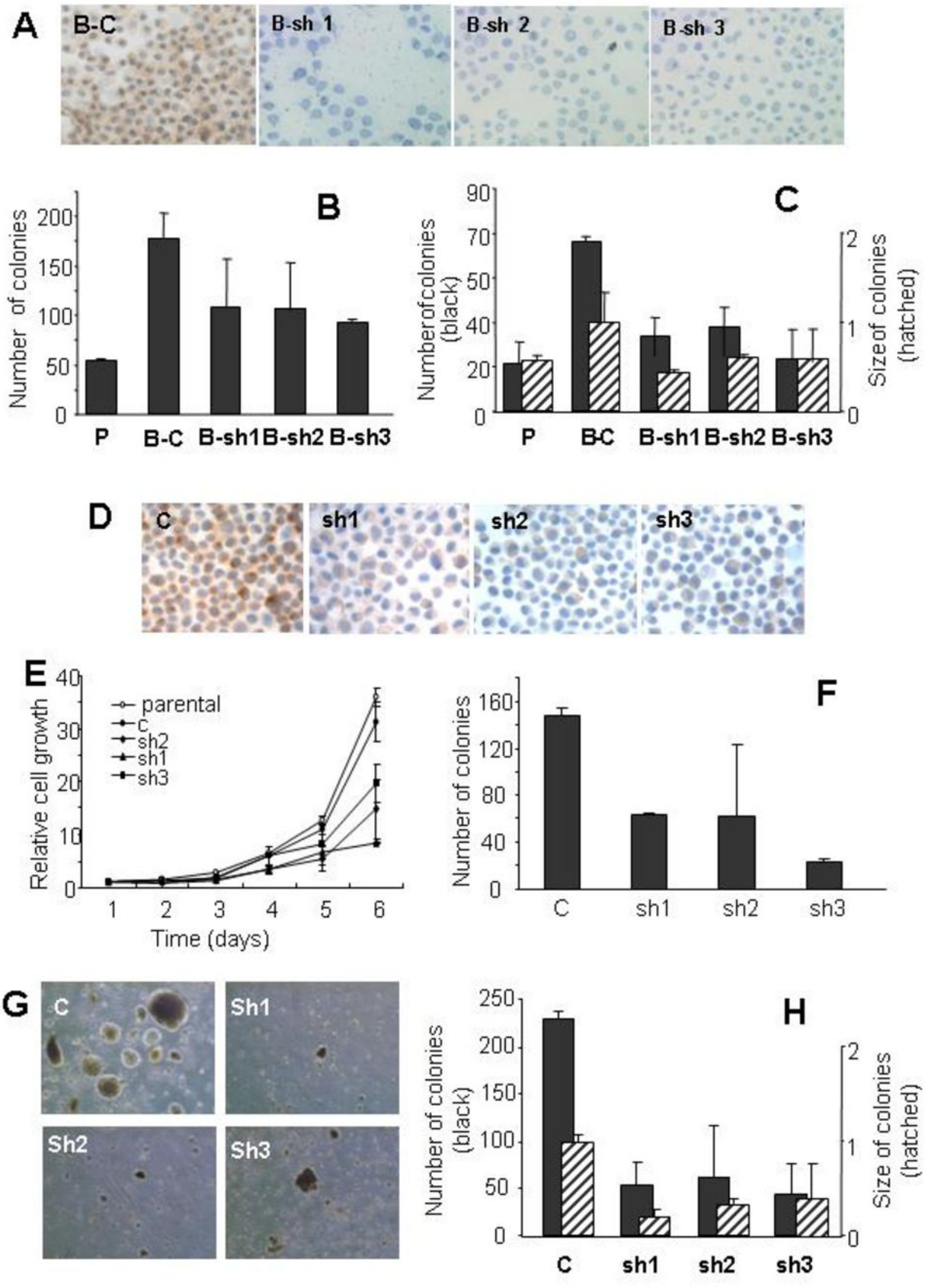
A
B-C
B-sh 1
B-sh 2
B-sh 3
B
Number of colonies
P
B-C
B-sh1
B-sh2
B-sh3
C
Number of colonies (black)
Size of colonies (hatched)
D
C
sh1
sh2
sh3
E
Relative cell growth
parental
C
sh2
sh1
sh3
Time (days)
F
Number of colonies
C
sh1
sh2
sh3
G
C
Sh1
Sh2
Sh3
H
Number of colonies (black)
Size of colonies (hatched)
C
sh1
sh2
sh3

Figure 4

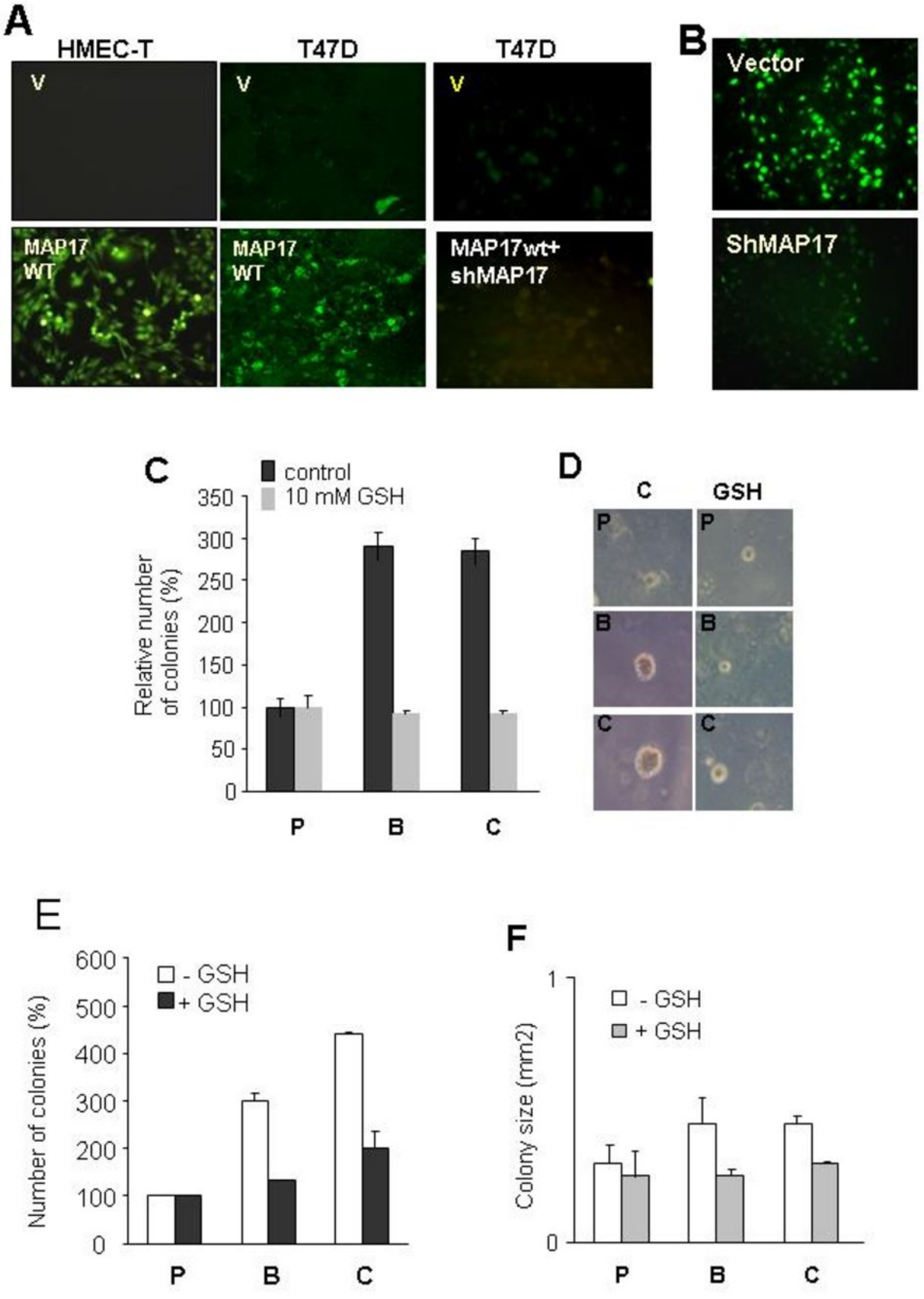
A
HMEC-T
T47D
T47D
V
V
V
MAP17 WT
MAP17 WT
MAP17wt+ shMAP17
B
Vector
ShMAP17
C
control
10 mM GSH
Relative number of colonies (%)
350
300
250
200
150
100
50
0
P
B
C
D
C
GSH
P
P
B
B
C
C
E
Number of colonies (%)
600
500
400
300
200
100
0
- GSH
+ GSH
P
B
C
F
Colony size (mm2)
1
0
- GSH
+ GSH
P
B
C

Figure 5

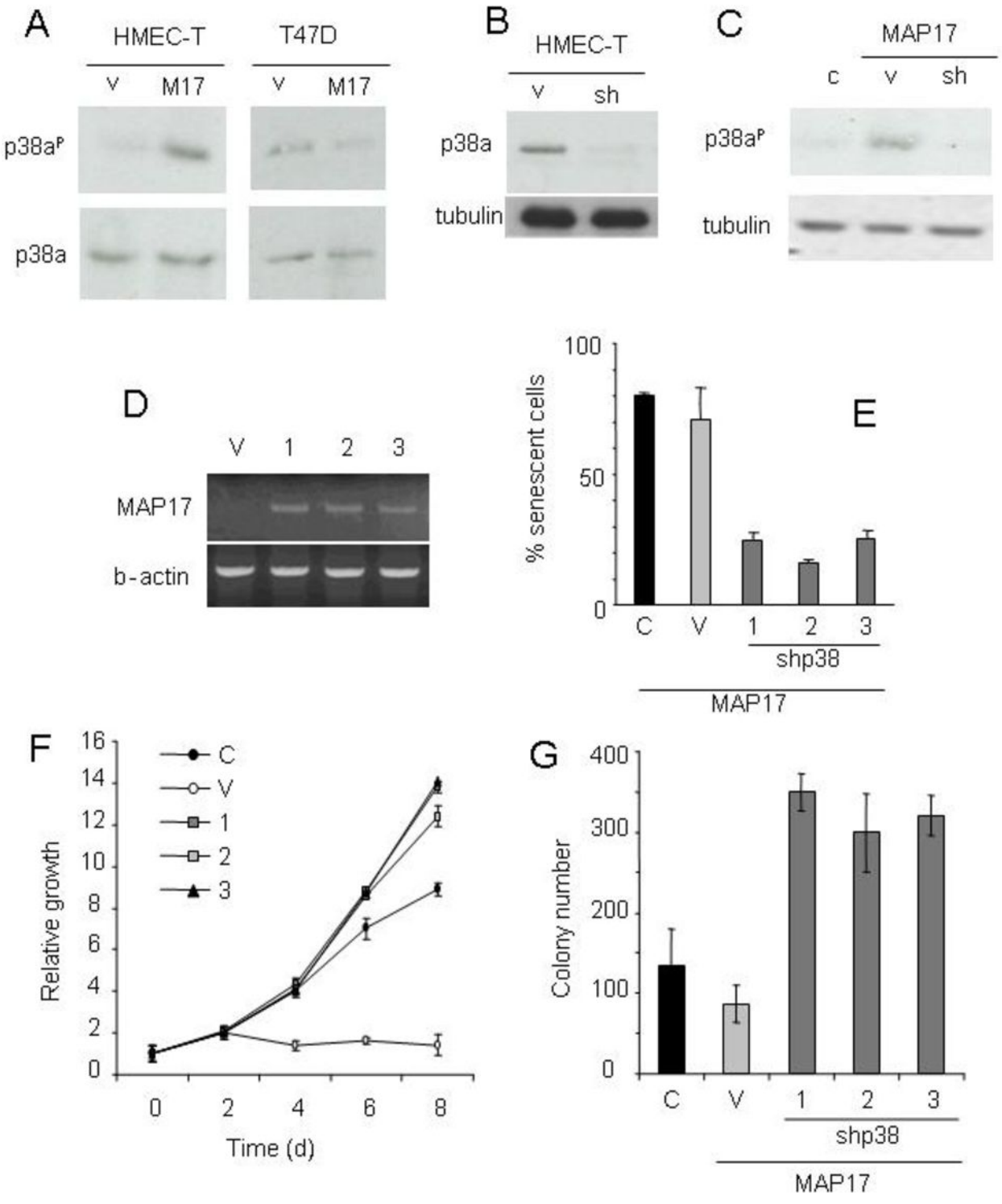
A
HMEC-T
T47D
V
M17
V
M17
p38a^P
p38a
B
HMEC-T
V
sh
p38a
tubulin
C
MAP17
c
V
sh
p38a^P
tubulin
D
V
1
2
3
MAP17
b-actin
E
% senescent cells
100
50
0
C
V
1
2
3
shp38
MAP17
F
Relative growth
16
14
12
10
8
6
4
2
0
C
V
1
2
3
0
2
4
6
8
Time (d)
G
Colony number
400
300
200
100
0
C
V
1
2
3
shp38
MAP17

Figure 6

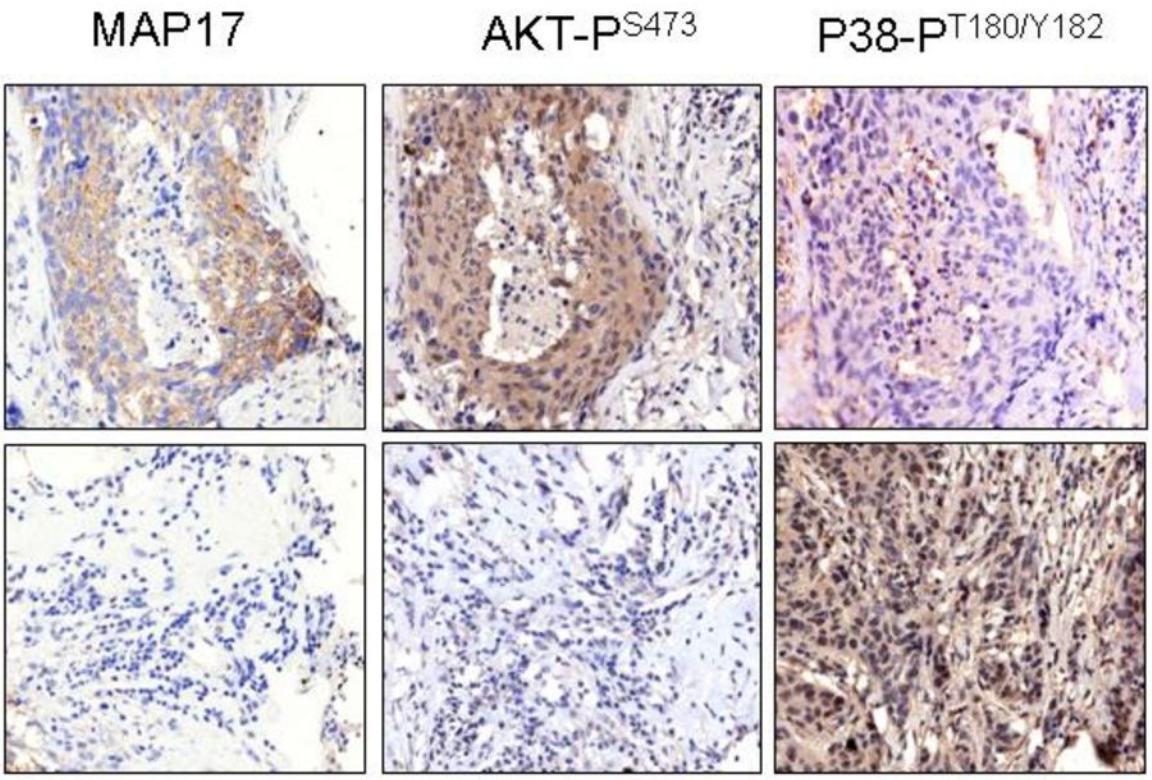
MAP17
AKT-P^{S473}
P38-P$^{T180/Y182}$

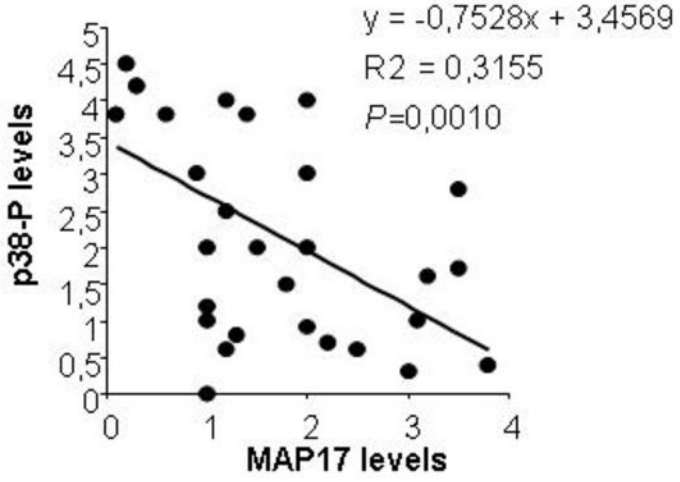
y = -0,7528x + 3,4569
R2 = 0,3155
P=0,0010
p38-P levels
MAP17 levels
0
0,5
1
1,5
2
2,5
3
3,5
4
4,5
5
0
1
2
3
4